

A 9-Connected Zirconium-Based Metal-Organic Framework for Ammonia Capture

Yongwei Chen,^{a,b} Xuan Zhang,^b Kaikai Ma,^b Zhijie Chen,^b Xingjie Wang,^{a,b} Julia Knapp,^b Selim Alayoglu,^c Fenfen Wang,^b Qibin Xia,^a Zhong Li,^a Timur Islamoglu,^b and Omar K. Farha^{*,b, d}

^aSchool of Chemistry and Chemical Engineering, South China University of Technology, Guangzhou 510640, P. R. China

^bDepartment of Chemistry and International Institute of Nanotechnology, Northwestern University, 2145 Sheridan Road, Evanston, Illinois 60208, United States

^cReactor Engineering and Catalyst Testing Core, Northwestern University, 2145 Sheridan Road, Evanston, Illinois 60208, United States

^dDepartment of Chemical and Biological Engineering, Northwestern University, 2145 Sheridan Road, Evanston, Illinois 60208, United States

Abstract

Construction of multifunctional metal-organic frameworks (MOFs) with asymmetric connectivity have the potential to expand the scope of their utilization. Herein, we report a robust 9-connected microporous Zr-based MOF, **NU-300**, assembled from asymmetric tri-carboxylate ligands and Zr₆ nodes. As indicated by single-crystal X-ray diffraction analysis, there exist uncoordinated carboxylate groups in the structure of **NU-300** that can participate in ammonia (NH₃) sorption through acid-base interactions which yield high uptake of NH₃ at low pressure regions (<0.01 bar). *In situ* infrared (IR) spectroscopy shows the interactions between Brønsted acidic sites and NH₃, which

suggests that **NU-300** can be used as a sorbent for NH₃ capture at low pressures.

Introduction

Metal-organic frameworks (MOFs) are a class of porous crystalline materials assembled by metal nodes and organic ligands.^{1, 2} Because of their high porosity,³ versatile pore structures,⁴ and tunable chemical functionalities,⁵⁻⁷ MOFs can be precisely designed at the molecular level for targeted applications including, but not limited to, gas storage⁸⁻¹⁰ and separation,¹¹⁻¹⁶ catalysis¹⁷⁻¹⁹, chemical sensing,^{20, 21} and more.^{22, 23} Particularly, zirconium-based MOFs (Zr-MOFs) have attracted extensive attention in recent years due to their high thermal and chemical robustness, as well as topological diversity.^{24, 25} Many reported Zr-MOFs contain 12-, 10-, 8-, 6- or 4-connected Zr₆ nodes with di-, tri-, and tetra-carboxylate ligands, showcasing different network topologies.²⁶ In designing stable zirconium MOFs, in general, highly symmetric di-, tri-, and tetra-carboxylate ligands are used which results in high symmetry MOFs when combined with symmetric Zr₆ nodes.^{24, 25} In the case of asymmetric ligands, although copper and rare-earth (RE) based MOFs have been constructed with non-planar tri-carboxylate ligands,^{27, 28} however, Zr-based MOFs have rarely been explored.²⁹ Asymmetric ligands can introduce new types of coordination environments and potentially unlock new topological structures for novel MOF materials.²⁷ Thus, the construction of Zr-MOFs with asymmetric ligands remains under explored for understanding the relationship between the different connected Zr₆ nodes and ligands within their unique structures, as well as exploiting the potential chemical properties related to the asymmetric ligands.

The exceptional stability of Zr-MOFs renders them as promising candidates for the capture of ammonia (NH₃).³⁰⁻³² Considering the associated corrosiveness and toxicity, the capture of NH₃ at extremely low concentrations using porous materials under ambient conditions in industrial settings is of great importance to comply with limits of short-term exposure (35 ppm) and long-term exposure (25 ppm) set by the Occupational Safety and Health Administration (OSHA).³¹ Several MOFs including HKUST-1,³³ MOF-74,³⁴ M(isonicotinic acid)₂ (M = Zn, Co, Cu, Cd),³⁵ MFM-300(Al),³⁶ M₂Cl₂BBTA (M = Co, Mn),³⁷ M₂Cl₂(BTDD) (M = Mn, Co, Ni and Cu),³⁸ and UiO-66 series^{30, 32} have been tested for NH₃ uptake. However, the majority of MOFs studied for NH₃ uptake showed structural degradation upon exposure or significant loss of uptake after consecutive cycles. So far, only a limited number of MOFs are reported to exhibit good reversible NH₃ sorption over multiple cycles, e.g. MFM-300(Al), Co₂Cl₂BBTA and M₂Cl₂(BTDD).³⁶⁻³⁸ The development of robust MOFs with reversible NH₃ sorption that can withstand multiple cycles remains challenging.

With the aforementioned challenges in mind, herein, we report a robust and functional 9-connected microporous Zr-MOF (**NU-300**) assembled from an asymmetric tri-carboxylate ligand and novel Zr₆ node with an unusual linker connectivity. Notably, **NU-300** has a high ammonia uptake at low pressures by exploiting Brønsted acidic sites on both the ligand and the node, which can be used as an adsorbent for NH₃ capture at low concentration.

Result and Discussion

The solvothermal reactions of ZrCl₄ and 3,5-di(4'-carboxylphenyl)benzoic acid

(H₃L) in N,N-dimethylformamide (DMF) with formic acid as a modulator, yielded colorless rhombic-shaped crystals of **NU-300** (NU stands for Northwestern University). Single crystal X-ray diffraction revealed that **NU-300** crystallizes in the orthorhombic *Imma* space group. The asymmetric unit of **NU-300** contains four Zr⁴⁺ atoms, each uniquely eight-coordinated. As shown in Figure 1a, Zr1 is coordinated by four distinct oxygen atoms from different carboxylates of four H₃L ligands and four μ_3 -O entities. Zr2 is coordinated by two distinct oxygen atoms from carboxylates of two H₃L ligands, one oxygen atom from formic acid, one oxygen atoms from DMF and four μ_3 -O entities. Zr3 is coordinated by three oxygen atoms from various carboxylates of three H₃L ligands, one oxygen from DMF and four μ_3 -O entities. Finally, Zr4 is coordinated by three oxygen atoms from various carboxylates of three H₃L ligands, one oxygen from terminal OH/H₂O and four μ_3 -O entities. Two Zr1, two Zr2, one Zr3 and one Zr4 atoms are connected together by eight μ_3 -O atoms to form the Zr₆O₈ cluster (Figure S2). This cluster differs from previously reported Zr₆ nodes that contain only one or two crystallographically independent Zr⁴⁺ atoms.^{26, 29, 39-42}

Moreover, the H₃L ligand adopts two types of coordination modes. In mode I, two carboxylate groups of H₃L adopt a bridging bis-monodentate mode while one is monodentate (Figure 1b). In mode II, two carboxylate groups of H₃L adopt monodentate and bridging bis-monodentate modes, respectively, while one carboxylate group remains uncoordinated (Figure 1c) and points to the channel along the *a*-axis in the 3D structure of **NU-300** (Figure 1d). The topological analysis indicates that **NU-300** consists of 9-connected Zr₆ nodes and three crystallographically independent

tridentate linkers, since monodentate carboxylic acids are not included in the connectivity counting. Thus, the 3D framework of **NU-300** can be simplified as a (3, 3, 3, 9)-connected network with a point symbol of $(4.6^2) (4^2.6)_2 (4^8.6^{20}.8^8)$ (Figure 1e), which is a new topology. The 9-connected Zr_6 nodes of **NU-300** are different from a previously reported 9-connect node, wherein the carboxylate ligands bridge adjacent Zr atoms in the node.²⁹

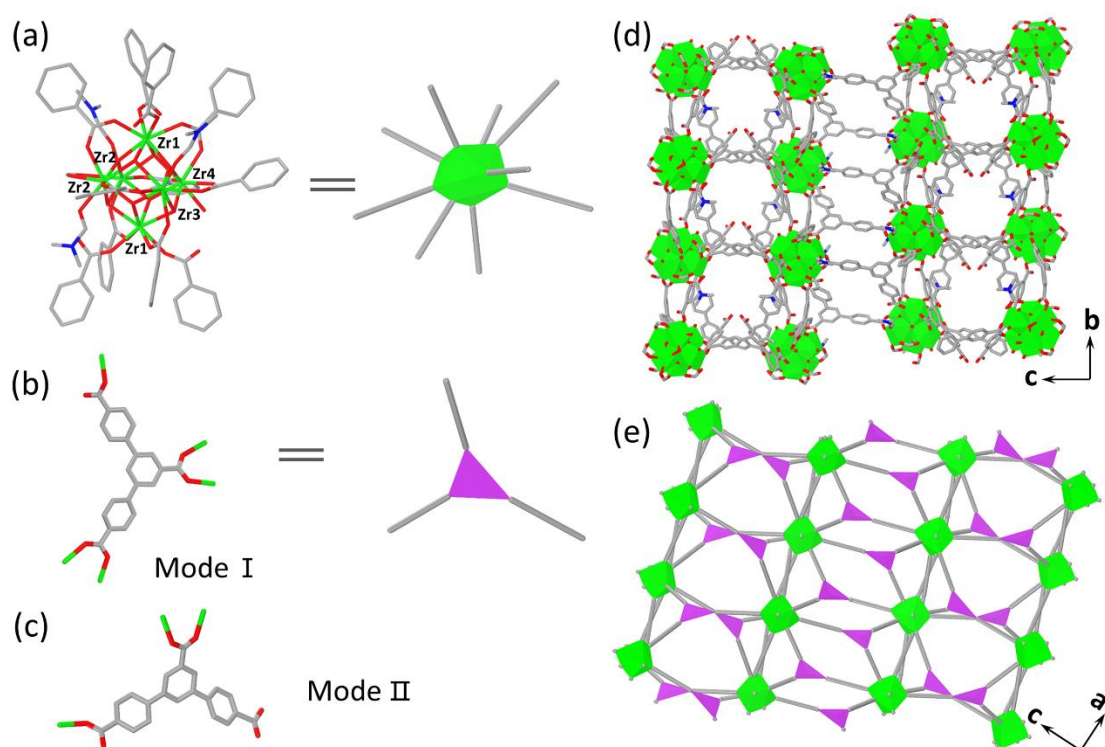


Figure 1. Single-crystal structure for **NU-300**: (a) Coordination environment of the node and schematic representation of each 9-connected Zr^{4+} . (b) Coordination mode I of the H_3L ligand and schematic representation of the 3-connected ligand. (c) Coordination mode II of the H_3L ligand. (d) The 3D structure of **NU-300** viewed along the *a* direction. (e) Schematic representation of the (3, 3, 3, 9)-connected networks of **NU-300** (Zr, green; C, grey; O, red).

The phase purity of bulk **NU-300** is confirmed by comparison of simulated and experimental PXRD patterns (Figure 2a). Thermogravimetric analysis (TGA) reveals that the framework of **NU-300** starts to decompose at around 400 °C in air (Figure S3), demonstrating the high thermal stability of **NU-300**. The permanent porosity of **NU-300** is confirmed by N₂ adsorption measurements at 77 K (Figure 2b). **NU-300** exhibits a type I isotherm, indicative of the microporous character of the material. The Brunauer-Emmett-Teller (BET) area and total pore volume for **NU-300** are calculated to be 1470 m²/g and 0.58 cm³/g, respectively, while the pore size distribution based on DFT modeling indicates micropores of ~11 Å (Figure 2b).

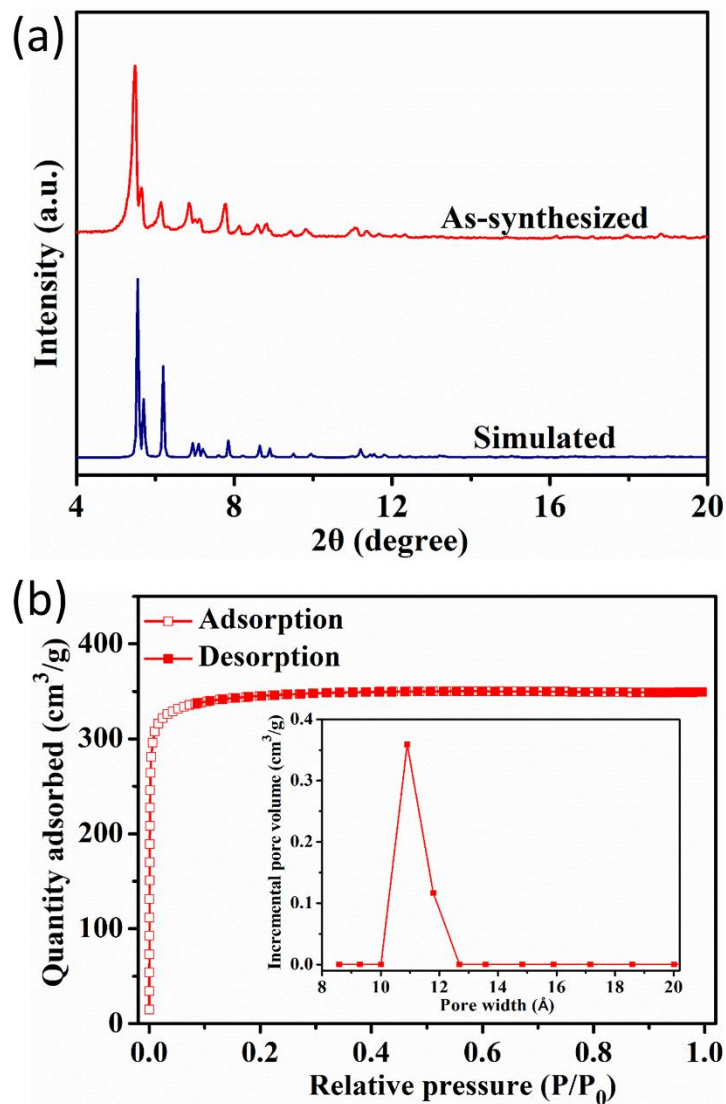


Figure 2. (a) PXR D patterns of the simulated and as-synthesized NU-300. (b) N₂ sorption isotherms at 77 K and DFT pore size distribution of NU-300.

The chemical stability of NU-300 is then investigated by soaking NU-300 in 100 °C H₂O, 0.01 M aqueous HCl (pH=2) and 0.001 M aqueous NaOH (pH=11) solutions for 24 h. As illustrated by PXR D patterns (Figure 3a), the crystallinity of the NU-300 is retained after these treatments. To further confirm the chemical stability of NU-300, N₂ sorption measurements are also conducted after these treatments (Figure 3b). The N₂ isotherms of NU-300 in hot water and acidic conditions are almost identical to that of

pristine NU-300, confirming its structural integrity and permanent porosity after exposure to boiling water and dilute acid. However, a decrease is observed in surface area and pore volume after base treatment.

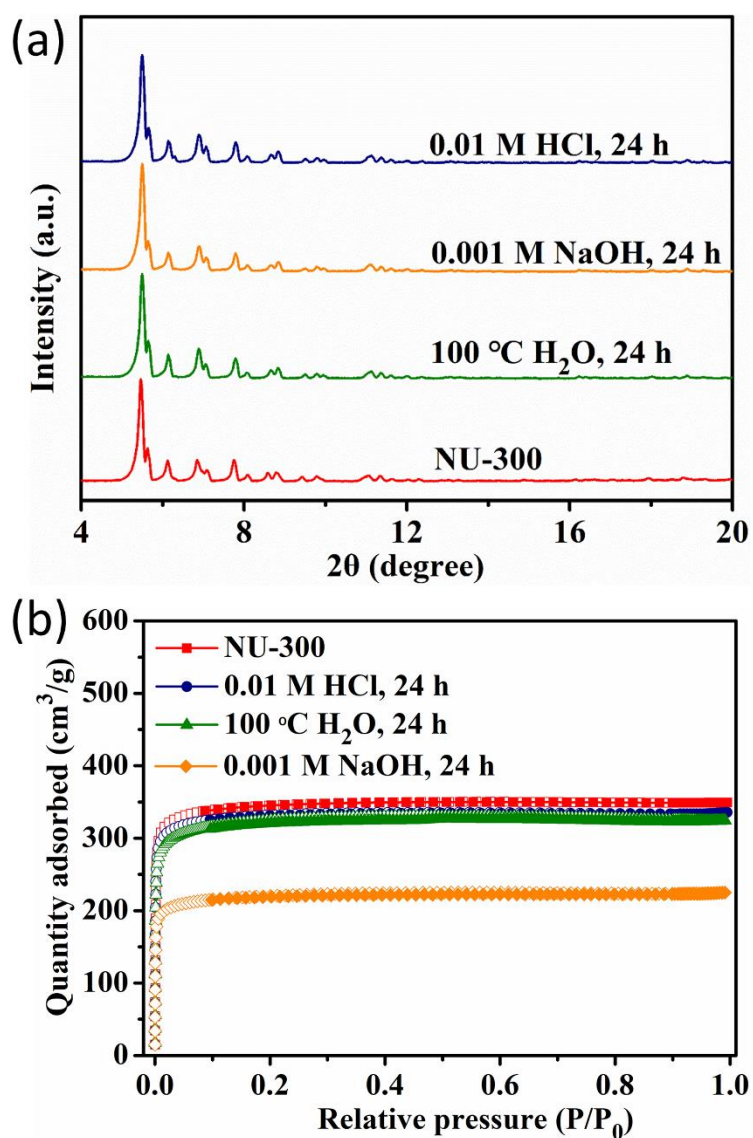


Figure 3. (a) PXRD patterns and (b) N₂ sorption isotherms at 77 K of NU-300 after treatment with 100 °C H₂O, 0.01 M HCl and 0.001 M NaOH for 24 h (open symbols, adsorption; solid symbols, desorption).

In light of the presence of free carboxylate groups (-COOH) within the framework, NH₃ sorption tests were conducted on NU-300 to investigate potential guest-host

interaction. The first run adsorption-desorption isotherm shows an adsorbed NH_3 amount of 8.28 mmol/g at 298 K and 1.0 bar (Figure 4a). At pressures less than 0.01 bar (Figure 4b), NH_3 molecules preferentially adsorbed to the Zr_6 nodes and Brønsted acidic sites of the free -COOH groups in **NU-300**, exhibiting the steep NH_3 isotherm. After regeneration at room temperature under vacuum, an NH_3 uptake of 3.30 mmol/g remained in **NU-300**, likely due to the chemisorption process by the formation of strong interactions between the uncoordinated -COOH groups and NH_3 molecules, apart from the acidic -OH groups on Zr_6 nodes (Figure S5). This indicates that Brønsted acid sites, particularly the free -COOH groups, aid **NU-300** in NH_3 uptake at low pressures, allowing **NU-300** to reach approximately 4 mmol/g uptake by 0.10 bar and 1.5 mmol/g by 0.01 bar, and the latter can be recycled for at least three times (Figure 4b). There was a loss in NH_3 uptake capacity at 1 bar between the first and second cycles while the third cycle of NH_3 sorption was nearly identical (5.71 and 5.41 mmol/g at 1.0 bar), suggesting that the loss in capacity occurs primarily in the initial sorption cycle.

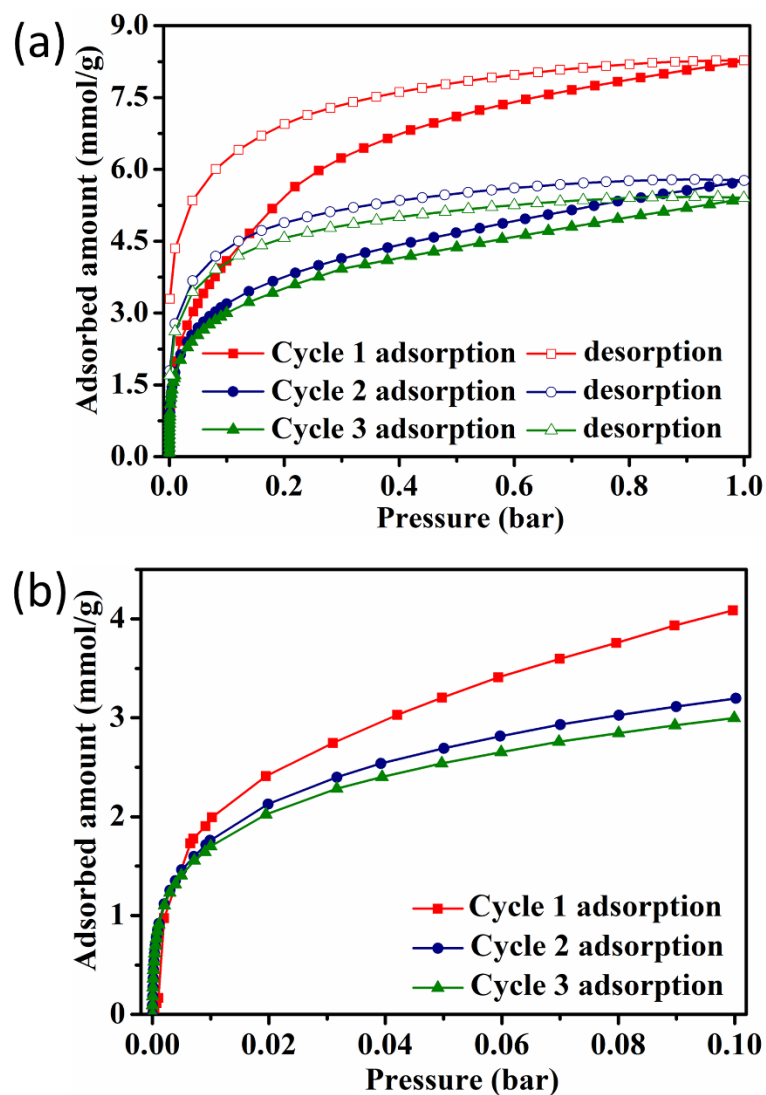


Figure 4. (a) Three cycle NH₃ sorption isotherms of NU-300 at 298 K and (b) low pressure range of 0-0.1 bar for clarity.

We then turned to IR spectroscopy to further assess how the carboxylic acid sites in NU-300 interact with NH₃ molecules during the adsorption and desorption processes. As observed in Figure 5, with NH₃ exposure for 60 min on NU-300, two characteristic NH₃ bands are observed, indicating NH₃ interactions with NU-300: the degenerate and symmetric deformation of NH₃ at 1625 and 1360 cm⁻¹, respectively.⁴³ The location of C=O stretching vibration of the free -COOH groups at 1730 cm⁻¹ (Figure S7) decreases

to 1710 cm^{-1} upon NH_3 exposure, possibly due to deprotonation and subsequent resonance that weakens the $\text{C}=\text{O}$ bond strength.⁴⁴ The appearance of overlapping bands between 3300 and 3700 cm^{-1} supports the deprotonation of $-\text{COOH}$ by NH_3 .⁴⁵ However, none of these bands between 3300 and 3700 cm^{-1} disappear upon Ar purge. NH_3 exposure also results in a new band at 1480 cm^{-1} , which could be assigned to the vibration of N-H in NH_4^+ .⁴³ These observations indicate that NH_3 molecules were protonated in acid-base reaction with Brønsted acidic sites. IR spectra showed that even after Ar purge residual adsorbed ammonia bands were still present which rationalized the loss in uptake between the first and second cycles.

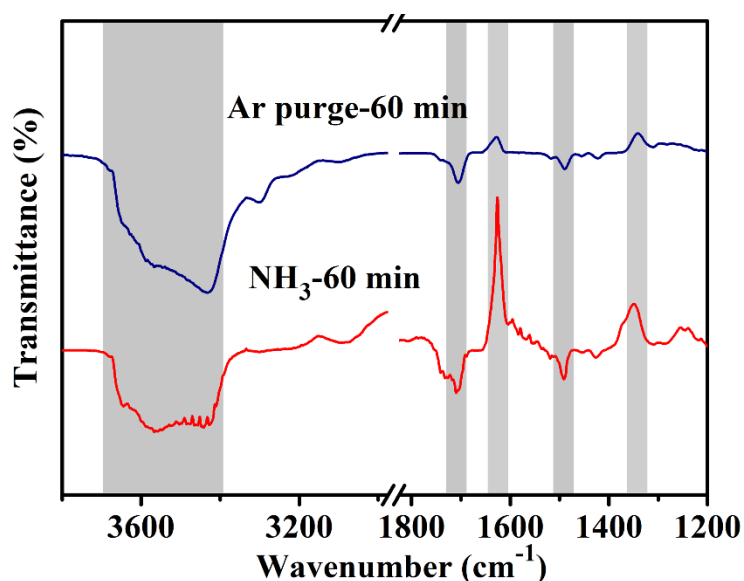


Figure 5. IR spectra of *in situ* NH_3 adsorption and desorption on NU-300 at 373 K with relevant bands highlighted in gray.

Conclusions

In summary, we have designed a robust 9-connected Zr-based MOF, NU-300 using an asymmetric tri-carboxylate ligand. The presence of free $-\text{COOH}$ groups on the ligands provides NU-300 with relevant functional properties for the chemisorption of NH_3

molecules at low partial pressures. For the first cycle adsorption, the adsorbed uptake of NH₃ was 8.28 mmol/g at 298 K and 1.0 bar. On the other hand, the second and third cycles of NH₃ sorption showed reduced NH₃ capacity compared to the first cycle, indicating saturation of the chemisorption of NH₃ in the first cycle. By *in situ* IR measurement of NH₃ adsorption and desorption, we observed that the ammonium band in the spectra which suggested the interactions between Brønsted acidic sites and NH₃ molecules. The chemical interaction of NH₃ and the framework indicated efficiency of introducing uncoordinated Brønsted acidic sites for achieving high NH₃ uptakes at low concentrations for air filtration applications.

ASSOCIATED CONTENT

Supporting Information

Crystallographic data for **NU-300** (CIF)

Materials synthesis and characterization, optical images of **NU-300** single crystals, crystallographic data for **NU-300**, Zr₆ node in **NU-300**, TGA curves, SEM images, DRIFTS spectrum, proton NMR spectra, IR spectra of *in situ* NH₃ adsorption and desorption on **NU-300** at 373 K

AUTHOR INFORMATION

Corresponding Author

*E-mail: o-farha@northwestern.edu

Notes

The authors declare no competing financial interest.

ACKNOWLEDGMENT

O. K. F. gratefully acknowledges support from the Defense Threat Reduction Agency (HDTRA1-19-1-0007). This work made use of the EPIC facility of Northwestern University's NUANCE Center, which has received support from the Soft and Hybrid Nanotechnology Experimental (SHyNE) Resource (NSF NNCI-1542205); the MRSEC program (NSF DMR-1720139) at the Materials Research Center; the International Institute for Nanotechnology (IIN); the Keck Foundation; and the State of Illinois, through the IIN. This work made use of the IMSERC at Northwestern University, which has received support from the NSF (CHE-1048773 and DMR-0521267); Soft and Hybrid Nanotechnology Experimental (SHyNE) Resource (NSF NNCI-1542205); the State of Illinois and International Institute for Nanotechnology (IIN). Y.C. gratefully acknowledges support from China Scholarship Council (CSC) during his visit to Northwestern University (201806150078). Q.X. gratefully acknowledges support from the National Natural Science Foundation of China (No. 21878101) for the synthesis of the linker.

REFERENCES

- (1) Zhou, H. C.; Long, J. R.; Yaghi, O. M., Introduction to metal-organic frameworks. *Chem. Rev.* **2012**, *112*, 673-4.
- (2) Kitagawa, S.; Kitaura, R.; Noro, S.-i., Functional porous coordination polymers. *Angew. Chem. Int. Ed.* **2004**, *43*, 2334-2375.
- (3) Farha, O. K.; Eryazici, I.; Jeong, N. C.; Hauser, B. G.; Wilmer, C. E.; Sarjeant, A. A.; Snurr, R. Q.; Nguyen, S. T.; Yazaydin, A. O.; Hupp, J. T., Metal-organic framework materials with ultrahigh surface areas: is the sky the limit? *J. Am. Chem. Soc.* **2012**, *134*, 15016-15021.

- (4) Liang, W.; Bhatt, P. M.; Shkurenko, A.; Adil, K.; Mouchaham, G.; Aggarwal, H.; Mallick, A.; Jamal, A.; Belmabkhout, Y.; Eddaoudi, M., A tailor-made interpenetrated MOF with exceptional carbon-capture performance from flue gas. *Chem* **2019**, *5*, 950-963.
- (5) Islamoglu, T.; Goswami, S.; Li, Z.; Howarth, A. J.; Farha, O. K.; Hupp, J. T., Postsynthetic tuning of metal-organic frameworks for targeted applications. *Acc. Chem. Res.* **2017**, *50*, 805-813.
- (6) Zhang, X.; Vermeulen, N. A.; Huang, Z.; Cui, Y.; Liu, J.; Krzyaniak, M. D.; Li, Z.; Noh, H.; Wasielewski, M. R.; Delferro, M.; Farha, O. K., Effect of redox “non-innocent” linker on the catalytic activity of copper-catecholate-decorated metal-organic frameworks. *ACS Appl. Mater. Interfaces* **2018**, *10*, 635-641.
- (7) Wang, Z.; Cohen, S. M., Postsynthetic modification of metal–organic frameworks. *Chem. Soc. Rev.* **2009**, *38*, 1315-1329.
- (8) Kundu, T.; Wahiduzzaman, M.; Shah, B. B.; Maurin, G.; Zhao, D., Solvent-induced control over breathing behavior in flexible metal-organic frameworks for natural-gas delivery. *Angew. Chem. Int. Ed.* **2019**, *58*, 8073-807.
- (9) Kapelewski, M. T.; Runčevski, T.; Tarver, J. D.; Jiang, H. Z. H.; Hurst, K. E.; Parilla, P. A.; Ayala, A.; Gennett, T.; FitzGerald, S. A.; Brown, C. M.; Long, J. R., Record high hydrogen storage capacity in the metal-organic framework Ni₂(m-dobdc) at near-ambient temperatures. *Chem. Mater.* **2018**, *30*, 8179-8189.
- (10) Wen, H.-M.; Li, B.; Li, L.; Lin, R.-B.; Zhou, W.; Qian, G.; Chen, B., A metal-organic framework with optimized porosity and functional sites for high gravimetric and volumetric methane storage working capacities. **2018**, *30*, 1704792.
- (11) Wang, H.; Li, J., Microporous metal-organic frameworks for adsorptive separation of C5-C6

alkane isomers. *Acc. Chem. Res.* **2019**, *52*, 1968-1978.

(12) Qazvini, O. T.; Babarao, R.; Shi, Z. L.; Zhang, Y. B.; Telfer, S. G., A robust ethane-trapping metal-organic framework with a high capacity for ethylene purification. *J. Am. Chem. Soc.* **2019**, *141*, 5014-5020.

(13) Chen, Y.; Qiao, Z.; Huang, J.; Wu, H.; Xiao, J.; Xia, Q.; Xi, H.; Hu, J.; Zhou, J.; Li, Z., Unusual moisture-enhanced CO₂ capture within microporous PCN-250 frameworks. *ACS Appl. Mater. Interfaces* **2018**, *10*, 38638-38647.

(14) Li, J.; Jiang, L.; Chen, S.; Kirchon, A.; Li, B.; Li, Y.; Zhou, H. C., Metal-organic framework containing planar metal-binding sites: efficiently and cost-effectively enhancing the kinetic separation of C₂H₂/C₂H₄. *J. Am. Chem. Soc.* **2019**, *141*, 3807-3811.

(15) Sen, S.; Hosono, N.; Zheng, J. J.; Kusaka, S.; Matsuda, R.; Sakaki, S.; Kitagawa, S., Cooperative bond scission in a soft porous crystal enables discriminatory gate opening for ethylene over ethane. *J. Am. Chem. Soc.* **2017**, *139*, 18313-18321.

(16) Wang, S. Q.; Mukherjee, S.; Patyk-Kazmierczak, E.; Darwish, S.; Bajpai, A.; Yang, Q. Y.; Zaworotko, M. J., Highly selective, high-capacity separation of o-xylene from C₈ aromatics by a switching adsorbent layered material. *Angew. Chem. Int. Ed.* **2019**, *58*, 6630-6634.

(17) Ding, M.; Flaig, R. W.; Jiang, H. L.; Yaghi, O. M., Carbon capture and conversion using metal-organic frameworks and MOF-based materials. *Chem. Soc. Rev.* **2019**, *48*, 2783-2828.

(18) Zhang, X.; Huang, Z.; Ferrandon, M.; Yang, D.; Robison, L.; Li, P.; Wang, T. C.; Delferro, M.; Farha, O. K., Catalytic chemoselective functionalization of methane in a metal-organic framework. *Nat. Catal.* **2018**, *1*, 356-362.

(19) Grigoropoulos, A.; McKay, A. I.; Katsoulidis, A. P.; Davies, R. P.; Haynes, A.; Brammer, L.;

Xiao, J.; Weller, A. S.; Rosseinsky, M. J., Encapsulation of crabtree's catalyst in sulfonated MIL-101(Cr): enhancement of stability and selectivity between competing reaction pathways by the MOF chemical microenvironment. *Angew. Chem. Int. Ed.* **2018**, *57*, 4532-4537.

(20) Mallick, A.; El-Zohry, A. M.; Shekhah, O.; Yin, J.; Jia, J.; Aggarwal, H.; Emwas, A. H.; Mohammed, O. F.; Eddaoudi, M., Unprecedented ultralow detection limit of amines using a thiadiazole-functionalized Zr(IV)-based metal-organic framework. *J. Am. Chem. Soc.* **2019**, *141*, 7245-7249.

(21) Zhang, X.; Saber, M. R.; Prosvirin, A. P.; Reibenspies, J. H.; Sun, L.; Ballesteros-Rivas, M.; Zhao, H.; Dunbar, K. R., Magnetic ordering in TCNQ-based metal-organic frameworks with host-guest interactions. *Inorg. Chem. Front.* **2015**, *2*, 904-911.

(22) Zhu, L.; Sheng, D.; Xu, C.; Dai, X.; Silver, M. A.; Li, J.; Li, P.; Wang, Y.; Wang, Y.; Chen, L.; Xiao, C.; Chen, J.; Zhou, R.; Zhang, C.; Farha, O. K.; Chai, Z.; Albrecht-Schmitt, T. E.; Wang, S., Identifying the recognition site for selective trapping of $^{99}\text{TcO}_4^-$ in a hydrolytically stable and radiation resistant cationic metal-organic framework. *J. Am. Chem. Soc.* **2017**, *139*, 14873-14876.

(23) Lin, C. G.; Zhou, W.; Xiong, X. T.; Xuan, W.; Kitson, P. J.; Long, D. L.; Chen, W.; Song, Y. F.; Cronin, L., Digital control of multistep hydrothermal synthesis by using 3D printed reactionware for the synthesis of metal-organic frameworks. *Angew. Chem. Int. Ed.* **2018**, *57*, 16716-16720.

(24) Yuan, S.; Qin, J. S.; Lollar, C. T.; Zhou, H. C., Stable metal-organic frameworks with group 4 metals: current status and trends. *ACS Cent. Sci.* **2018**, *4*, 440-450.

(25) Chen, Z.; Hanna, S. L.; Redfern, L. R.; Alezi, D.; Islamoglu, T.; Farha, O. K., Reticular chemistry in the rational synthesis of functional zirconium cluster-based MOFs. *Coord. Chem. Rev.* **2019**, *386*, 32-49.

- (26) Zhang, Y.; Zhang, X.; Lyu, J.; Otake, K. I.; Wang, X.; Redfern, L. R.; Malliakas, C. D.; Li, Z.; Islamoglu, T.; Wang, B.; Farha, O. K., A flexible metal-organic framework with 4-connected Zr_6 nodes. *J. Am. Chem. Soc.* **2018**, *140*, 11179-11183.
- (27) Schnobrich, J. K.; Lebel, O.; Cychosz, K. A.; Dailly, A.; Wong-Foy, A. G.; Matzger, A. J., Linker-directed vertex desymmetrization for the production of coordination polymers with high porosity. *J. Am. Chem. Soc.* **2010**, *132*, 13941-13948.
- (28) Wang, Y.; Feng, L.; Fan, W.; Wang, K. Y.; Wang, X.; Wang, X.; Zhang, K.; Zhang, X.; Dai, F.; Sun, D.; Zhou, H. C., Topology exploration in highly connected rare-earth metal-organic frameworks via continuous hindrance control. *J. Am. Chem. Soc.* **2019**, *141*, 6967-6975.
- (29) He, T.; Zhang, Y. Z.; Kong, X. J.; Yu, J.; Lv, X. L.; Wu, Y.; Guo, Z. J.; Li, J. R., Zr(IV)-based metal-organic framework with T-shaped ligand: unique structure, high stability, selective detection, and rapid adsorption of $Cr_2O_7^{2-}$ in Water. *ACS Appl. Mater. Interfaces* **2018**, *10*, 16650-16659.
- (30) Mounfield, W. P.; Taborga Claire, M.; Agrawal, P. K.; Jones, C. W.; Walton, K. S., Synergistic effect of mixed oxide on the adsorption of ammonia with metal-organic frameworks. *Ind. Eng. Chem. Res.* **2016**, *55*, 6492-6500.
- (31) DeCoste, J. B.; Peterson, G. W., Metal-organic frameworks for air purification of toxic chemicals. *Chem. Rev.* **2014**, *114*, 5695-5727.
- (32) Chen, Z.; Wang, X.; Noh, H.; Ayoub, G.; Peterson, G. W.; Buru, C. T.; Islamoglu, T.; Farha, O. K., Scalable, room temperature, and water-based synthesis of functionalized zirconium-based metal-organic frameworks for toxic chemical removal. *CrystEngComm* **2019**, *21*, 2409-2415.
- (33) Katz, M. J.; Howarth, A. J.; Moghadam, P. Z.; DeCoste, J. B.; Snurr, R. Q.; Hupp, J. T.; Farha, O. K., High volumetric uptake of ammonia using Cu-MOF-74/Cu-CPO-27. *Dalton Trans.* **2016**, *45*,

4150-4153.

(34) Grant Glover, T.; Peterson, G. W.; Schindler, B. J.; Britt, D.; Yaghi, O., MOF-74 building unit has a direct impact on toxic gas adsorption. *Chem. Eng. Sci.* **2011**, *66*, 163-170.

(35) Chen, Y.; Shan, B.; Yang, C.; Yang, J.; Li, J.; Mu, B., Environmentally friendly synthesis of flexible MOFs $M(\text{NA})_2$ ($M = \text{Zn}, \text{Co}, \text{Cu}, \text{Cd}$) with large and regenerable ammonia capacity. *J. Mater. Chem. A* **2018**, *6*, 9922-9929.

(36) Godfrey, H. G. W.; da Silva, I.; Briggs, L.; Carter, J. H.; Morris, C. G.; Savage, M.; Easun, T. L.; Manuel, P.; Murray, C. A.; Tang, C. C.; Frogley, M. D.; Cinque, G.; Yang, S.; Schroder, M., Ammonia storage by reversible host-guest site exchange in a robust metal-organic framework. *Angew. Chem. Int. Ed.* **2018**, *57*, 14778-14781.

(37) Rieth, A. J.; Dinca, M., Controlled gas uptake in metal-organic frameworks with record ammonia sorption. *J. Am. Chem. Soc.* **2018**, *140*, 3461-3466.

(38) Rieth, A. J.; Tulchinsky, Y.; Dinca, M., High and reversible ammonia uptake in mesoporous azolate metal-organic frameworks with open Mn, Co, and Ni sites. *J. Am. Chem. Soc.* **2016**, *138*, 9401-9404.

(39) Feng, D.; Wang, K.; Su, J.; Liu, T. F.; Park, J.; Wei, Z.; Bosch, M.; Yakovenko, A.; Zou, X.; Zhou, H. C., A highly stable zeotype mesoporous zirconium metal-organic framework with ultralarge pores. *Angew. Chem. Int. Ed.* **2015**, *54*, 149-154.

(40) Yuan, S.; Lu, W.; Chen, Y. P.; Zhang, Q.; Liu, T. F.; Feng, D.; Wang, X.; Qin, J.; Zhou, H. C., Sequential linker installation: precise placement of functional groups in multivariate metal-organic frameworks. *J. Am. Chem. Soc.* **2015**, *137*, 3177-3180.

(41) Furukawa, H.; Gandara, F.; Zhang, Y. B.; Jiang, J.; Queen, W. L.; Hudson, M. R.; Yaghi, O. M.,

Water adsorption in porous metal-organic frameworks and related materials. *J. Am. Chem. Soc.* **2014**, *136*, 4369-4381.

(42) Wang, H.; Dong, X.; Lin, J.; Teat, S. J.; Jensen, S.; Cure, J.; Alexandrov, E. V.; Xia, Q.; Tan, K.; Wang, Q.; Olson, D. H.; Proserpio, D. M.; Chabal, Y. J.; Thonhauser, T.; Sun, J.; Han, Y.; Li, J., Topologically guided tuning of Zr-MOF pore structures for highly selective separation of C6 alkane isomers. *Nat. Commun.* **2018**, *9*, 1745.

(43) Micek-Ilnicka, A.; Gil, B.; Lalik, E., Ammonia sorption by Dawson acid studied by IR spectroscopy and microbalance. *J. Mol. Struct.* **2005**, *740*, 25-29.

(44) Yang, Y.; Faheem, M.; Wang, L.; Meng, Q.; Sha, H.; Yang, N.; Yuan, Y.; Zhu, G., Surface pore engineering of covalent organic frameworks for ammonia capture through synergistic multivariate and open metal site approaches. *ACS Cent. Sci.* **2018**, *4*, 748-754.

(45) Petit, C.; Seredych, M.; Bandosz, T. J., Revisiting the chemistry of graphite oxides and its effect on ammonia adsorption. *J. Mater. Chem.* **2009**, *19*, 9176-9185.

Table of Contents (TOC) Graphic

